

1 **Silencing *SmDI* in Solanaceae alters susceptibility to root-knot nematodes**

2

3 Joffrey Mejias¹, Yongpan Chen^{1,2}, Nhat-My Truong^{1,3}, Karine Mulet¹, Stéphanie Jaubert-

4 Possamai¹, Pierre Abad¹, Bruno Favery^{1,*} and Michaël Quentin^{1,*}

5

6 ¹ INRAE, Université Côte d'Azur, CNRS, ISA, F-06903 Sophia Antipolis, France

7 ² Department of Plant Pathology and Key Laboratory of Pest Monitoring and Green

8 Management of the Ministry of Agriculture, China Agricultural University, 100193 Beijing,

9 China

10 ³ Graduate School of Science and Technology, Kumamoto University, Kumamoto 860-11

11 8555, Japan

12

13 * Correspondence (Tel 33492386495; bruno.favery@inrae.fr or michael.quentin@inrae.fr).

14

15 ORCID IDs: 0000-0003-3323-1852 (B.F.); 0000-0002-8030-1203 (M.Q.)

16

17 **Keywords:** *Meloidogyne*, Pathogen, Effector, Susceptibility gene, Nucleolus, Spliceosome,

18 *Solanum lycopersicum*, *Nicotiana benthamiana*

19

20 SHORT TITLE (max 40 cha.) *SmDI*, a susceptibility gene to nematodes

21

22 The author responsible for distributing materials integral to the findings presented in this

23 article is: Michael Quentin michael.quentin@inrae.fr.

24

25 **Word count:** 5306 words (Introduction, 814; Results, 1376; Discussion, 1528; Experimental
26 procedures, 1360; Acknowledgements, 228). **Figures:** 6. **Supporting information files:** 6 (2
27 tables and 4 figures).

28

29 **Summary**

30 Root-knot nematodes (RKNs) are among the most damaging pests of agricultural crops.
31 Indeed, *Meloidogyne* is an extremely polyphagous genus of nematodes that can infect
32 thousands of plant species. A few genes for resistance (R-genes) to RKNs suitable for use in
33 crop breeding have been identified, and new virulent strains and species of nematode emerge
34 rendering these R-genes ineffective. Effective parasitism is dependent on the secretion, by the
35 RKN, of effectors targeting plant functions, which mediate the reprogramming of root cells
36 into specialised feeding cells. These cells, the giant cells, are essential for RKN development
37 and reproduction. The EFFECTOR 18 protein (EFF18) from *M. incognita* interacts with the
38 spliceosomal protein SmD1 in Arabidopsis, disrupting its function in alternative splicing
39 regulation and modulating the giant cell transcriptome. We show here that EFF18 is a
40 conserved RKN-specific effector. We also show here that EFF18 effectors also target SmD1
41 in *Nicotiana benthamiana* and *Solanum lycopersicum*. The alteration of *SmD1* expression by
42 virus-induced gene silencing (VIGS) in Solanaceae affects giant cell formation and nematode
43 development. Thus, *SmD1* is a susceptibility gene and a promising target for the development
44 of broad resistance, especially in Solanaceae, for the control of *Meloidogyne* spp.

45

46 **Introduction**

47 Plant parasitic nematodes are major crop pests causing crop losses of several million dollars
48 annually, through damage to almost all cultivated plants, and the transmission of plant viruses
49 (Singh et al., 2013). Root-knot nematodes (RKNs) of the genus *Meloidogyne* are considered
50 to be the most detrimental of these plant parasites, due to the magnitude of the economic
51 losses they cause (Jones *et al.*, 2013). RKNs are widespread worldwide and can infect more
52 than 5,500 different plant species, including many species of major agricultural interest.
53 About 100 RKN species have been described, and those reproducing asexually by mitotic
54 parthenogenesis (*M. incognita*, *M. javanica*, *M. arenaria* and *M. enterolobii*) are the most
55 polyphagous and damaging pests. By contrast, those reproducing sexually or by meiotic
56 parthenogenesis (*M. hapla*) have a smaller host range (Blok et al., 2008; Castagnone-Sereno,
57 2006).

58 All RKNs are sedentary endoparasites that induce the formation of specialised feeding
59 structures and typical root deformations, known as galls or root knots, that deprive the plant of
60 nutrients (Escobar *et al.*, 2015; Favery *et al.*, 2016). After hatching from eggs, the stage 2
61 juveniles (J2) of *M. incognita* penetrate the root apex and migrate between plant cells to reach
62 the plant vascular system (Holbein *et al.*, 2019). Once there, the filiform J2 switch to a
63 sedentary lifestyle, by selecting five to seven cells of the vascular parenchyma and inducing
64 their reprogramming into specialised feeding cells, known as giant cells (Escobar *et al.*, 2015;
65 Favery *et al.*, 2016; Olmo *et al.*, 2020). These hypertrophied and multinucleate cells act as
66 metabolic sinks close to the xylem and phloem vessels that withdraw water and nutrients from
67 the sap (Rodiuc *et al.*, 2014). The nematode uses these specific giant cells for feeding for the
68 rest of its life. After successive moults, the sedentary swollen juveniles develop into an adult
69 female that lays her egg masses on the root surface, thus completing the cycle. The giant cells
70 are hypertrophied and multinucleate, harbouring hundreds of nuclei. They are produced by

71 successive nuclear divisions uncoupled from cytokinesis, followed by nuclear
72 endoreduplication (de Almeida Engler and Gheysen, 2013). RKN induce giant cells and gall
73 formation by recruiting the developmental pathways of post-embryonic organogenesis and
74 regeneration to promote transient pluripotency (Olmo *et al.*, 2020).

75 RKNs parasitise plants and induce the redifferentiation of vascular cells into giant cells by
76 secreting effectors, molecules that recruit/hijack plant functions (Mejias *et al.*, 2019; Toruño
77 *et al.*, 2016). RKN effectors, particularly those produced by the three oesophageal gland cells
78 and secreted into the host through a stylet, are involved in the four main functions underlying
79 parasitism: (i) the degradation and modification of plant cell walls during J2 migration within
80 the root; (ii) the suppression of host defences; (iii) the reprogramming of plant vascular cells
81 as giant cells and (vi) the maintenance of these feeding sites (Mitchum *et al.*, 2013; Truong *et*
82 *al.*, 2015). The profound morphological and metabolic changes associated with giant cell
83 induction by RKNs and the transcriptional reprogramming occurring during the formation of
84 these cells require the secretion of effectors targeting key nuclear functions (Hewezi and
85 Baum, 2013; Quentin *et al.*, 2013). With the exception of plant cell wall-degrading enzymes
86 (Danchin *et al.*, 2010), very few effectors have been shown to be conserved and functional in
87 multiple RKN species. For example, 16D10 encodes a conserved secretory peptide conserved
88 in five RKN species (*M. incognita*, *M. arenaria*, *M. hapla*, *M. javanica*, *M. chitwoodi*) that
89 stimulates root growth and functions as a ligand for a putative plant transcription factor
90 (Huang *et al.*, 2006; Dinh, 2015). The silencing of *16D10* by RNA interference methods
91 confers broad resistance to RKNs (Huang *et al.*, 2006; Dinh, 2015). The chorismate mutases,
92 MiCM3 (Wang *et al.*, 2018) and MjCM1 (Doyle and Lambert, 2003), and the transthyretin-
93 like proteins, MjTTL5 (Lin *et al.*, 2016) and MhTTL2 (Gleason *et al.*, 2017), also appear to
94 be effectors conserved among RKNs. Interestingly, MhTTL2 is expressed in the amphids
95 (Gleason *et al.*, 2017), whereas MjTTL5 is expressed specifically in the subventral glands,

96 suggesting different roles for these two molecules in parasitism, encoded by the same gene
97 family (Lin *et al.*, 2016).

98 We recently showed that MiEFF18, a nuclear effector from *M. incognita*, is secreted *in*
99 *planta*, targets the giant cell nuclei and interacts with the SmD1 protein, a core component of
100 the spliceosome (Mejias *et al.*, 2020). We show here that MiEFF18 is a specific and
101 conserved RKN effector and that orthologous genes are specifically expressed in the salivary
102 glands of RKNs. We also show that MiEFF18 and its orthologue in *M. enterolobii*, MeEFF18,
103 interact with SmD1 proteins from different plant species. Moreover, virus-induced gene
104 silencing (VIGS) approaches silencing the SmD1 genes of *N. benthamiana* and *S.*
105 *lycopersicum* greatly impair RKN infection. These results are consistent with the targeting, by
106 RKNs, of conserved spliceosomal functions, to drive the development of giant cells,
107 facilitating parasitism on a large spectrum of host plants.

108

109 **Results**

110 **EFF18 is a conserved RKN-specific effector targeting plant nucleus**

111 MiEFF18 was first described in the *M. incognita* genome (Mejias *et al.*, 2020; Nguyen *et al.*,
112 2018; Rutter *et al.*, 2014). Database queries showed that MiEFF18 displayed no sequence
113 homology or known domains, and that it was absent from nematodes of other genera, such as
114 cyst nematodes and free-living nematodes. By contrast, EFF18 orthologues were identified in
115 seven of the eight RKNs for which genome sequences were available: *M. incognita*, *M.*
116 *javanica*, *M. arenaria* (Blanc-Mathieu *et al.*, 2017), *M. hapla* (Opperman *et al.*, 2008), *M.*
117 *enterolobii* (syn. *M. mayaguensis*) (Koutsovoulos *et al.*, 2020), *M. floridensis* (Lunt *et al.*,
118 2014) and *M. luci* (Susič *et al.*, 2020) (Figure 1, Table S1, Figure S1). No EFF18 orthologue
119 was identified in *M. graminicola* (Somvanshi *et al.*, 2018). Three paralogous copies were
120 identified, in the *M. incognita*, *M. javanica* and in *M. luci* genomes. Four copies were detected

121 in *M. arenaria* and a single copy was detected in *M. hapla*, *M. floridensis* and *M. enterolobii*.
122 A sequence alignment and analysis of the RKN EFF18 protein sequences showed that they
123 were more than 60% identical, between 279 and 316 amino acids (aa) long and that they had
124 an N-terminal secretion signal peptide (SSP), a low-complexity acidic D/E-rich region and a
125 C-terminal lysine (K)-rich domain carrying direct repeats (Figure 1a, Figure S2). Only the C-
126 terminal K-rich domain displayed marked differences between copies.

127 A phylogenetic tree based on an alignment of the 17 RKN EFF18 protein sequences
128 showed divergences between copies among the same species (Figure 1a). EFF18 proteins
129 more closely related to MiEFF18a/Minc18636 harboured one monopartite NLS and one
130 bipartite NLS, whereas other copies are more divergent (*e.g.* MiEFF18b/Minc15401 and
131 MiEFF18c) and contained only one monopartite NLS (Figure 1a). MiEFF18a fused at its C-
132 or N-terminus to GFP (green fluorescent protein) and MeEFF18a fused at its N-terminus to
133 GFP were transiently expressed in *Nicotiana benthamiana* leaf epidermis. For EFF18
134 constructs, GFP fluorescence was only detected in the nucleus, with a strong GFP signal
135 accumulating in the nucleolus (Figure 1b). In contrast, GFP alone was detected in the
136 cytoplasm and the nucleus, but not in the nucleolus (Figure 1b). The EFF18s with bipartite
137 NLS were 98% to 100% identical to the MiEFF18a protein, whereas those with only
138 monopartite NLS were only 79 to 89% identical to this protein (Figure 1c). *M. hapla* had the
139 most divergent genome of the *Meloidogyne* species tested. It was found to have a single copy
140 of the gene, 63-65% identical to the closest copies and the most divergent copies, which
141 suggests that the ancestor of RKN species had an EFF18 gene, and providing support for the
142 role of EFF18 as a conserved effector.

143

144 **RKN EFF18s are specifically expressed in the subventral glands**

145 MiEFF18 have been shown to be more strongly expressed at parasitic stages and to be
146 expressed specifically in the subventral glands of *M. incognita* J2s (Rutter et al., 2014;
147 Nguyen et al., 2018; Mejias et al., 2020). We studied the pattern of expression of genes
148 encoding orthologous sequences of MiEFF18 in two other RKN species, by performing *in situ*
149 hybridisation (ISH) for the *M. enterolobii* *MeEFF18a* and the *M. arenaria* *MaEFF18a*
150 sequences. A specific signal was detected in the subventral oesophageal gland cells of pre-J2s
151 after hybridisation with digoxigenin-labelled *MeEFF18a* and *MaEFF18a* antisense probes
152 (Figure 2). No signal was detected in pre-J2s with sense negative controls. This finding
153 suggests that *MaEFF18a* and *MeEFF18a*, may, like *MiEFF18a*, be secreted and play an
154 important role in nematode parasitism.

155

156 **MiEFF18a and MeEFF18a interact with the SmD1 proteins of *A. thaliana*, *N.***
157 ***benthamiana* and *S. lycopersicum***

158 We have demonstrated an interaction between MiEFF18 and the nuclear ribonucleoproteins
159 SmD1s from *S. lycopersicum* and *A. thaliana*, modulating the pattern of alternative splicing
160 and promoting the formation of giant cells (Mejias et al., 2020). Two genes, *AtSmD1a*
161 (AT3G07590) and *AtSmD1b* (AT4G02840), encode SmD1 proteins in *Arabidopsis* (Koncz et
162 al., 2012) and two genes encode 100% identical SmD1 proteins (SlSmD1) in *S. lycopersicum*:
163 *SlSmD1a* (Soly06g084310) and *SlSmD1b* (Soly09g064660). In *N. benthamiana*, we
164 identified three genes encoding SmD1s: *NbSmD1a* (*Niben101Scf01782g05006*), *NbSmD1b*
165 (*Niben101Scf05290g01011*), and *NbSmD1c* (*Niben101Scf04283g03011*). A multiple sequence
166 alignment showed that SmD1 was highly conserved in these species, with 93% identity
167 between SlSmD1 and the sequence from which it diverged most strongly, *AtSmD1b* (Figure
168 3a). Like all Sm proteins, SmD1s carry two conserved Sm motifs mediating protein-protein
169 interactions during small nuclear ribonucleoprotein (snRNP) biogenesis (Figure 3b). We

170 investigated the subcellular localisation of SmD1 in plant cells, by transiently expressing
171 constructs encoding GFP-SmD1 fusion proteins in *N. benthamiana*. We confirmed a strong
172 accumulation of SlSmD1a and AtSmD1b in the nucleolus and in Cajal bodies, and a weaker
173 accumulation in the nucleoplasm (Figure 3c).

174 We then investigated whether MeEFF18a was also able to interact with SmD1 proteins
175 from *S. lycopersicum* and *A. thaliana*, like MiEFF18 (Mejias et al., 2020). Using a pairwise
176 yeast-two hybrid approach, we showed that MiEFF18a and MeEFF18a interact with SmD1
177 proteins from plants of different clades, such as *A. thaliana*, *S. lycopersicum* and *N.*
178 *benthamiana* (Figure 3d). As a control, we tested SmD1 interactions with another *M.*
179 *incognita* effector, MiEFF16, encoded by the *Minc16401* gene and expressed in the
180 subventral glands, with the same nuclear location *in planta* as MiEFF18 (Mejias et al., 2020).
181 No interaction was observed between MiEFF16 and SmD1 proteins in yeast (Figure 3d).
182 These results demonstrate that EFF18 proteins are conserved among RKNs and that they
183 interact with SmD1 proteins, which are conserved among plant species.

184

185 ***SmD1* acts as a susceptibility gene for infection in plants of different clades**

186 We recently demonstrated an important role for the AtSmD1b protein in giant cell formation
187 and successful nematode infection (Mejias et al., 2020). We investigated whether *SmD1* is a
188 conserved susceptibility gene required to ensure infection, and essential for RKN parasitism
189 in Solanaceae species, by using a virus-induced gene silencing (VIGS) approach to alter the
190 expression of *SmD1* genes in *S. lycopersicum* and *N. benthamiana*.

191 We first performed a VIGS assay to silence *SmD1* genes in *S. lycopersicum* (Figure 4a). We
192 evaluated silencing efficiency by RT-qPCR on emerging leaves. Treated tomatoes had much
193 lower levels of *SmD1* transcripts (Figure 4b). Tomatoes in which SmD1 genes were silenced
194 displayed developmental defects on emerging leaves and had a shorter root system (Figure
195 S3). In tomato plants infected with *M. incognita*, in which *SmD1* genes were silenced, the

196 number of females producing egg masses was much smaller than that in control plants treated
197 with the TRV-GFP virus (Figure 4c).

198 Because of adverse effect of *SmDI* silencing on development in tomato, we then silenced
199 the *SmDI* genes in *N. benthamiana*, which allows performing a VIGS assay at a later
200 developmental stage when roots have already developed substantially (Figure 5a and 5b). An
201 evaluation of silencing efficiency by RT-qPCR showed that *N. benthamiana* roots subjected
202 to VIGS had much lower levels of *SmDI* transcripts, particularly for the most strongly
203 expressed gene, *NbSmDIb* (Figure 5c). We observed no significant decrease in the expression
204 of the two mostly weakly expressed genes, *NbSmDIa* and *NbSmDIc* (Figure 5c; Figure S4).
205 *N. benthamiana* plants in which *SmDI* was silenced produced a much smaller number of galls
206 (up to 80% fewer) following infection with *M. incognita* (Figure 5d).

207 We studied the effect on nematode and giant cell development in detail, by investigating
208 J2s *in planta* by the fuchsine acid staining method, to determine the proportions of migrating
209 filiform and sedentary swollen parasitic juveniles and their ratio. The percentage of migrating
210 filiform J2s was higher (90%) in plants in which *SmDI* was silenced, which had a lower
211 percentage of swollen juveniles, indicating a defect in the RKN development (Figure 6a). We
212 also investigated whether the giant cells formed on plants in which *SmDI* was silenced
213 displayed developmental defects. We observed these cells directly, under a confocal
214 microscope, after clearing in benzyl alcohol/benzyl benzoate (BABB ; Cabrera et al., 2018). A
215 comparison of the mean surface areas of the largest giant cells in each gall showed that giant
216 cells from plants in which *SmDI* was silenced were 36% smaller than those from control
217 plants (Figure 6b and 6c). These results confirm the important role of *SmDI* in giant cell
218 formation in Solanaceae species and the requirement of this protein for successful nematode
219 development.

220

221 **Discussion**

222 The ability of plant pathogens to infect their hosts is generally dependent on the secretion of
223 effectors. Most pathogens secrete effectors to overcome host physical defences, such as the
224 plant cell wall, and to suppress plant immune responses (Toruño *et al.*, 2016). Other effectors
225 are more specific to the parasitic strategy of the pathogen and may regulate host gene
226 expression or trigger changes in host cell morphology and physiology to allow pathogen
227 feeding and development. Most obligatory biotrophs form specific feeding structures, such as
228 the haustoria of biotrophic filamentous pathogens, and produce sets of specific effectors
229 (Chaudhari *et al.*, 2014; O’Connell and Panstruga, 2006). RKNs are root endoparasites that
230 manipulate host cells to form specialised giant cells for feeding. These giant cells constitute
231 the sole source of nutrients for the nematode, and are, therefore, essential for nematode
232 survival. RKNs induce giant cells by manipulating root cell developmental programmes.
233 Indeed, massive transcriptomic reprogramming occurs during giant cell formation (Favery *et*
234 *al.*, 2016; Mitchum *et al.*, 2013). Genes associated with root meristem function, lateral root
235 formation and the establishment of the vasculature, in particular, are tightly regulated upon
236 giant cell induction (Cabrera *et al.*, 2014; Olmo *et al.*, 2020; Yamaguchi *et al.*, 2017).
237 Alternative splicing has recently been shown to occur in *Arabidopsis* following infection with
238 *M. incognita*, and this process contributes to transcriptome and proteome diversity (Mejias *et*
239 *al.*, 2020).

240

241 **EFF18 is a nuclear conserved RKN-specific effector**

242 Nuclear effectors are thought to mediate the transcriptional reprogramming required for giant
243 cell formation (Mejias *et al.*, 2019; Quentin *et al.*, 2013). They may interfere with the function
244 of transcription factors, as described for Mi16D10, which interacts with SCARECROW-like
245 transcription factors (Huang *et al.*, 2006), or may themselves act as transcription factors, as

246 reported for Mi7H08 (Zhang *et al.*, 2015). MiEFF18 is another RKN effector that has been
247 shown to be secreted within host cells, in which it localises to the nucleus. MiEFF18 has been
248 shown to interact with the SmD1 protein, a core component of the spliceosome conserved in
249 all eukaryotes, thereby modulating alternative splicing and gene expression (Mejias *et al.*,
250 2020). MiEFF18 may corrupt the function of *Arabidopsis SmD1* function to modulate the
251 expression of various genes encoding proteins involved in giant cell formation through
252 processes such as DNA replication or cytokinesis (Mejias *et al.*, 2020). We show here that the
253 manipulation of SmD1 function by MiEFF18 plays a key role in giant cell development in
254 other plant species, such as *Nicotiana benthamiana* and the tomato *Solanum lycopersicum*.

255 Genes encoding the MiEFF18 effector were found in all available *Meloidogyne* spp.
256 genomes other than the draft genome for the rice RKN *M. graminicola* (Somvanshi *et al.*,
257 2018). EFF18 is exclusive to RKN, being absent from all other parasitic nematodes and other
258 plant pathogens with parasitic strategies not involving the induction of giant feeding cells. At
259 least one orthologous copy of a MiEFF18 sequence was detected in each of the available
260 *Meloidogyne* genomes, demonstrating that MiEFF18 is a conserved effector. The multiple
261 copies identified in *M. incognita*, *M. javanica* and *M. arenaria* are consistent with the
262 polyploidy of these mitotic parthenogenetic species (Koutsovoulos *et al.*, 2020). The absence
263 of an EFF18 effector in *M. graminicola* may be explained by the particular host range and life
264 cycle of this nematode. *M. graminicola* may have lost the EFF18 effector during
265 specialisation on monocotyledonous hosts and adaptation to the infection of submerged roots
266 (Mantelin *et al.*, 2017). These growing conditions may have resulted in different requirements
267 for the modulation of gene expression for giant cell ontogenesis, dependent on effectors other
268 than EFF18.

269 The distribution of EFF18 orthologues in two major groups, with copies (e.g. MiEFF18a)
270 carrying two NLS, and those of the most divergent group (e.g. MiEFF18b) carrying only one

271 NLS, suggested a possible duplication of the ancestral MiEFF18 gene in the ancestor of RKN
272 species, with one of the duplicated genes either gaining or losing a bipartite NLS. The
273 proteins from the closest group to the MiEFF18a gene would be expected to function
274 similarly to MiEFF18a, through the modulation of SmD1 functions, due to the very high level
275 of sequence identity between these proteins (98% identity). *M. enterolobii* is an extremely
276 polyphagous species that reproduces through mitotic parthenogenesis, like *M. incognita*.
277 Therefore, we investigated the functionality of proteins MeEFF18 orthologue. We found that,
278 like MiEFF18, MeEFF18a was able to interact with SmD1 proteins from *A. thaliana*, *N.*
279 *benthamiana* and *S. lycopersicum*, suggesting that orthologous copies of MiEFF18a are
280 functional and target the same functions in different host plants. MiEFF18a and MeEFF18a
281 are the first examples of conserved RKN effectors able to target the same conserved plant
282 process in different plant species.

283

284 **Targeting conserved effectors to engineer plant resistance**

285 The identification of conserved effectors could lead to new strategies for developing broad
286 resistance (Huang *et al.*, 2006; Landry *et al.*, 2020; Peeters *et al.*, 2013; Roux *et al.*, 2015).
287 Only a few RKN effectors have been described to be conserved. The MAP (*Meloidogyne*
288 avirulence protein) effector family, which includes *M. incognita* Mi-MAP1.2, was shown to
289 be conserved in 13 of the 21 RKN species tested, and absent from other genera of plant-
290 parasitic nematodes (PPNs) (Tomalova *et al.*, 2012). The genes of the MAP effector family
291 harbour one or multiple CLE-like motifs, which may be involved in feeding site formation, as
292 demonstrated for cyst nematode CLE-like peptides, which promote syncytium formation
293 (Rutter *et al.*, 2014; Mitchum *et al.*, 2012). MjNULG1a, from *M. javanica*, is a nuclear
294 effector with a demonstrated role in parasitism. Southern blot experiments have revealed the
295 presence of MjNULG1a orthologues in *M. incognita* and *M. enterolobii*, but not in other

296 PPNs (Lin *et al.*, 2013). Similarly, the 16D10 effector is exclusive to RKNs (Huang *et al.*,
297 2006; Dinh, 2015). The use of host-induced gene silencing (HIGS) approaches to engineer
298 plant resistance to RKNs has excited considerable interest (Ali *et al.*, 2017; Banerjee *et al.*,
299 2017). The targeting of genes involved in nematode development or encoding effectors has
300 been considered. Silencing conserved effectors may allow specific resistance to RKNs with
301 no impact on non-targeted species. Studies of Mi16D10 have demonstrated the feasibility of
302 conferring RKN resistance in *Arabidopsis*, potato or grape through the targeting of this
303 effector (Huang *et al.*, 2006; Yang *et al.*, 2013; Dinh, 2015). However, this strategy is
304 constrained both by limited HIGS effectiveness, by the redundancy of the effector's function
305 and the difficulty in targeting the point in time when the effector plays a key role in the
306 interaction.

307

308 **Targeting essential conserved effector targets to induce a loss of susceptibility**

309 The use of resistant cultivars or rootstocks is an efficient and non-polluting method for
310 controlling RKNs. Very few natural resistance genes (R-genes) have been identified to date,
311 in a limited number of plant species. Furthermore, some RKN species or populations are not
312 controlled by these genes, e.g. *M. enterolobii* (Elling, 2013; Kiewnick *et al.*, 2009) or can
313 overcome these resistances, e.g. populations of *M. incognita* virulent against tomato *Mi1.2*
314 (Castagnone-Sereno, 2006). One alternative would be to target conserved plant genes
315 encoding proteins involved in host processes that are hijacked by the biotrophic pathogens for
316 settlement and feeding, and that are essential for disease development. These susceptibility
317 genes (S-genes) represent an alternative to R-genes for the deployment of pathogen resistance,
318 and they may be more durable in the field (Dong and Ronald, 2019; Engelhardt *et al.*, 2018;
319 van Schie and Takken, 2014). Well-characterised examples of S-genes include the genes
320 encoding eukaryotic translation initiation factors, the sugar transporter SWEET14 or PMR6,

321 which are required for viral, bacterial and oomycete infections, respectively (Langner *et al.*,
322 2018; van Schie and Takken, 2014; Schmitt-Keichinger, 2019).

323 In recent decades, transcriptomic approaches have been widely used to identify genes
324 regulated upon RKN infection, and, thus, host functions manipulated by RKNs. However, as
325 thousands of genes are differentially regulated during a compatible interaction, the
326 identification of S-genes from these data is a very time-consuming process, probably
327 explaining why only a few genes to date have been shown to be important for the
328 establishment of giant cells (Favery *et al.*, 2016). Interactomics approaches have recently been
329 used to identify the direct plant targets manipulated by PPN effectors. Only a few targets of
330 RKN effectors have been identified, but most have been shown to be instrumental in
331 promoting nematode parasitism (Mejias *et al.*, 2019). SmD1 is a host target of an effector
332 required for host susceptibility to RKNs in several plant clades. It exerts a conserved plant
333 function targeted by a core effector in *Arabidopsis* and Solanaceae, common to diverse
334 *Meloidogyne* species that have adopted the same successful parasitic strategy based on the
335 induction of giant feeding cells in the root in several host species. SmD1 is thus a good
336 candidate S-gene for targeting in the engineering of crop resistance to RKN. As SmD1
337 functions is required for plant development knockout mutations of this gene have adverse
338 effects, it will be necessary to identify mutant alleles that can evade recognition by MiEFF18
339 whilst remaining competent to perform the functions of SmD1 in the regulation of plant
340 development in a continually changing environment. This strategy has proven to be effective
341 for potyvirus susceptibility *eIF4E* genes (Bastet *et al.*, 2019).

342

343 **Experimental procedures**

344 **Nematode and plant materials**

345 *M. incognita* (Morelos strain), *M. arenaria* (Guadeloupe strain) and *M. enterolobii* (Godet
346 strain) were multiplied on tomato (*Solanum lycopersicum* cv. “Saint Pierre”) growing in a
347 growth chamber (25°C, 16 h photoperiod). Freshly hatched J2s were collected as previously
348 described (Caillaud and Favery, 2016). For VIGS experiments, *Nicotiana benthamiana* and
349 *Solanum lycopersicum* (cv M82) seeds were sown on soil and incubated at 4°C for two days.
350 After germination, *N. benthamiana* and tomato plantlets were transplanted into pots
351 containing soil and sand (1:1), and were grown at 24°C and 16°C, respectively (photoperiod,
352 16 h: 8 h, light: dark).

353

354 **Sequence analysis, alignment and phylogenetic tree**

355 The sequences of EFF18 paralogues and orthologues were obtained from *Meloidogyne*
356 genomic resources http://www6.inra.fr/meloidogyne_incognita and Wormbase parasite.
357 Protein sequences were aligned with the MAFFT tool on the EBI server
358 (<https://www.ebi.ac.uk/Tools/msa/mafft/>). The alignment was then used as input for the
359 IQTree Web server <http://iqtree.cibiv.univie.ac.at/> (Trifinopoulos et al., 2016) to generate the
360 maximum likelihood phylogenetic tree. The model chosen by the inbuilt model test was
361 HIVb+F+G4. Support for the nodes was calculated with 100 bootstrap replicates. *M. hapla*
362 was used as the outgroup in the phylogenetic tree for MiEFF18 orthologues. The tree was
363 visualised in iTOL <https://itol.embl.de/>. The sequence alignment were coloured with
364 Boxshade (https://embnet.vital-it.ch/software/BOX_form.html). The pairwise sequence
365 identity matrix of RKN EFF18 protein sequences was generated with Sequence Demarcation
366 Tool version 1.2 software (Muhire *et al.*, 2014) (<http://web.cbio.uct.ac.za/~brejnev/>).

367

368 ***In situ* hybridisation (ISH)**

369 ISH was performed on freshly hatched *M. arenaria* and *M. enterolobii* pre-J2s, as previously
370 described (Jaouannet *et al.*, 2018). The MaEFF18, and MeEFF18 gene fragments were

371 amplified with specific primers (Table S2). A sense probe for MeEFF18 was used as a
372 negative control. Images were obtained with a microscope (Zeiss Axioplan2, Germany).

373

374 **Pairwise yeast two-hybrid assays**

375 For pairwise yeast two-hybrid (Y2H) assays, the coding sequences (CDS) of the MiEFF16,
376 MiEFF18 and MeEFF18 effectors without their secretion signals were amplified (Table S1)
377 and inserted into pB27 as C-terminal fusions with LexA. Full-length SmD1 CDS sequences
378 (*SlSmD1*, *NbSmD1* and *AtSmD1b*) were amplified (Table S1) and inserted into pP6 as C-
379 terminal fusions with Gal4-AD. The pB27 and pP6 constructs were verified by sequencing
380 and used to transform the L40 Δ Gal4 (MAT α) and Y187 (MAT α) yeast strains, respectively.
381 Y187 and L40 Δ Gal4 were crossed and diploids were selected on medium lacking tryptophan
382 and leucine. Interactions were investigated on medium lacking tryptophan, leucine and
383 histidine and supplemented with 0.5 mM 3-aminotriazole (3-AT).

384

385 ***N. benthamiana* agroinfiltration**

386 Transient expression was achieved by infiltrating *N. benthamiana* leaves with *A. tumefaciens*
387 GV3101 strains harbouring GFP-fusions, as previously described (Caillaud *et al.*, 2008).
388 Leaves were imaged 48 hours after agroinfiltration, with an inverted confocal microscope
389 equipped with an argon ion and HeNe laser as the excitation source. For simultaneous GFP
390 imaging, samples were excited at 488 nm and GFP emission was detected selectively with a
391 505-530 nm band-pass emission filter.

392

393 **Virus-induced gene silencing in Solanaceae**

394 VIGS assays were performed on *N. benthamiana* and *S. lycopersicum*. We used the Sol
395 Genomics Network VIGS-Tool (<https://vigs.solgenomics.net/>) to design the best sequence for

396 silencing *SlSmD1a* transcripts, and selected the full-length *SlSmD1a* (without the ATG and
397 STOP codons) for amplification by PCR with the TRV2-*SlSmD1*-F/TRV2-*SlSmD1*-R primer
398 pairs (Table S2). The PCR products were digested with *EcoRI* and *XhoI* and ligated to the
399 tobacco rattle virus RNA 2 vector (TRV2) for the transformation of *A. tumefaciens* strain
400 GV3101. VIGS assays were performed, as previously described, by the co-infiltration of
401 leaves of three-week-old *N. benthamiana* plants (Lange *et al.*, 2013; Velasquez *et al.*, 2009)
402 or 10-days-old tomato plants (Cox *et al.*, 2019) with agrobacterial strains containing the RNA
403 1 vector (TRV1) and TRV2. Tomato plants were incubated at 16°C for four weeks. Three
404 independent biological replicates were established for each set of conditions ($n = 15$ per
405 replicate). Two *N. benthamiana* root systems per set of conditions and per replicate, or *S.*
406 *lycopersicum* leaves were collected upon RKN infection and frozen in liquid nitrogen for
407 subsequent RNA extraction and the assessment of silencing efficiency by RT-qPCR.

408

409 **RKN infection assay, juveniles in the plant and giant cell area measurements**

410 *N. benthamiana* plants subjected to VIGS were inoculated with 200 *M. incognita* J2s per
411 plant, 10 days post inoculation (dpi) with TRV, and incubated at 24°C. *S. lycopersicum* plants
412 subjected to VIGS were inoculated with 150 *M. incognita* J2s per plant, 30 dpi with TRV, and
413 incubated at 16°C for two weeks before transfer to 24°C. *N. benthamiana* infected roots were
414 collected two weeks after infection whereas *S. lycopersicum* infected roots were collected six
415 weeks after infection. Galls, and egg masses stained with 4.5% eosin were counted under a
416 binocular microscope, and root system was weighted ($n=12$ to 19 and $n=18$ to 21 plants per
417 replicates for *N. benthamiana* and *S. lycopersicum*, respectively). Three and two independent
418 biological replicates were established for each set of conditions in *N. benthamiana* and *S.*
419 *lycopersicum*, respectively. The impact of the plant lines on the number of galls per mg of
420 root in *N. benthamiana* and the number of egg masses per plant in *S. lycopersicum* were

421 analyzed using Kruskal Wallis test since the dependent variable did not follow a Normal
422 distribution using a Shapiro-Wilk Test. The different replicates of the numbers of galls per mg
423 of roots in *N. benthamiana* were pooled for the analyzes because there was no difference
424 between the replications ($X^2_2= 2.8$, $P = 0.248$). By contrast, the different replicates of the
425 number of egg masses per plant in *S. lycopersicum* varied depending on the replication ($X^2_1=$
426 5.3 , $P = 0.022$), and they were analyzed separately. Thus, both the number of galls per mg of
427 root in *N. benthamiana* and the number of egg masses per plant in *S. lycopersicum* varied
428 significantly between the two plant lines tested ($X^2_1= 57.2$, $P < 0.001$; $X^2_1 > 25.6$, $P < 0.001$,
429 respectively). For determination of the ratio of filiform-to-swollen nematodes, infected roots
430 were collected 14 dpi, parasitic nematodes were stained with fuchsine acid, as previously
431 described (Karssen and Moens, 1983), and nematodes were examined under a binocular
432 microscope (model LSM 880; Zeiss) ($n= 3$ plants per replicate for TRV-empty lines and $n = 5$
433 plants per replicate for TRV-SmD1 lines, with a mean of 75 nematodes observed per
434 condition and per replicate). Three independent biological replicates were established for each
435 set of conditions. Statistical analyses were carried out with R software (R Development Core
436 Team, version 3.1.3). For giant cell area measurements, galls were cleared in BABB, as
437 previously described (Cabrera *et al.*, 2018), and examined under an inverted confocal
438 microscope (model LSM 880; Zeiss). The mean areas of the biggest giant cell in each gall
439 from *N. benthamiana*, for each genotype, were measured with Zeiss ZEN software ($n = 32$
440 and 26 galls for control and SmD1-VIGSed plants, respectively). One biological experiment
441 was performed for giant cells measurement. The data were analysed with a *t*-test since the
442 data followed a normal distribution ($t = 3.5$, $P < 0.001$).

443

444 **Reverse transcription-quantitative PCR**

445 We assessed silencing efficiency in Solanaceae species, by extracting total RNA with TriZol
446 (Invitrogen) and subjecting 1 µg of total RNA to reverse transcription with the Superscript IV
447 reverse transcriptase (Invitrogen). qPCR analyses were performed as described by Nguyen et
448 al., 2016. Primers were designed to amplify both SlSmD1 transcripts or to discriminate
449 between the three copies of SmD1 present in *N. benthamiana* specifically according to their
450 UTR, to prevent the amplification of TRV2-SlSmD1 constructs (Table S2). We performed
451 RT-qPCR in triplicate on cDNA samples from three independent biological replicates. The
452 *EF-1α* and Actin genes were used for the normalisation of RT-qPCR data (Liu *et al.*, 2012).
453 Quantifications and statistical analyses were performed with SATqPCR (Rancurel *et al.*,
454 2019), and the results are expressed as normalised absolute quantities.

455

456 **Graphs and statistical analysis**

457 Graphs and plots were created with Microsoft® Office Excel® 2016 and statistical
458 calculations were performed in R.

459

460 **Accession numbers**

461 The sequence data from this article can be found in the *Arabidopsis* Information Resource
462 (<https://www.arabidopsis.org/>), Solgenomics (<https://solgenomics.net/>) and/or
463 GenBank/EMBL databases. All RKN EFF18 protein sequences are presented in the Figure S1
464 The accession numbers are summarised in Table S1 including MiEFF18a (KX907770),
465 MeEFF18a (MW272456), NbSmD1a (MT683762), NbSmD1b (MT683763) and NbSmD1c
466 (MT683764).

467

468 **Acknowledgements**

469 We thank Dr Johnathan Dalzell and Steven Dyer (Queen's University Belfast, UK) for tomato
470 VIGS protocol and vectors, Pr S.P. Dinesh-Kumar (University of California, Davis, USA) for
471 VIGS vectors and Hybrigenics Services (Paris, France) for providing the pB27 and pP6
472 vectors and the L40 Δ Gal4 and Y187 yeast strains. We thank Dr Nemo Peeters and Dr Laurent
473 Deslandes (LIPM, Castanet Tolosan, France) and Gregori Bonnet (Syngenta seeds) for helpful
474 discussions. Microscopy work was performed at the SPIBOC imaging facility of Institut
475 Sophia Agrobiotech. We thank Dr Lucie S. Monticelli for providing the statistical analyses.
476 We thank Dr Olivier Pierre and the whole platform team for their help with microscopy. This
477 work was funded by the INRAE SPE department and the French Government (National
478 Research Agency, ANR) through the 'Investments for the Future' LabEx SIGNALIFE:
479 programme reference #ANR-11-LABX-0028-01, by the INRA-Syngenta Targetome project,
480 by the French-Japanese bilateral collaboration programmes PHC SAKURA 2016 #35891VD
481 and 2019 #43006VJ and by the French-Chinese bilateral collaboration program PHC XU
482 GUANGQI 2020 #45478PF. J.M. holds a doctoral fellowship from the French *Ministère de*
483 *l'Enseignement Supérieur, de la Recherche et de l'Innovation* (MENRT grant). N.M.T. was
484 supported by a USTH fellowship, as part of the 911-USTH programme of the Ministry of
485 Education and Training of The Socialist Republic of Vietnam. Y.P.C. obtained scholarships
486 from the China Scholarship Council (No. 201806350108) for studies at INRAE, France.

487

488 **Conflict of interest**

489 The authors have no conflict of interest to declare.

490

491 **Author contributions**

492 J.M. designed and performed experiments, and interpreted data; J.M., YC and N.M.T.
493 generated constructs and performed yeast two-hybrid analysis; YC performed *in situ*

494 hybridisation and *in planta* subcellular localisation experiments; KM performed VIGS in
495 tomato and nematode infection tests; J.M., P.A., S.J.P., B.F. and M.Q. wrote the manuscript;
496 B.F. and M.Q. obtained funding, designed the work and supervised the experiments and data
497 analyses; all the authors read and edited the manuscript.

498

499 **References**

500

501 Ali, M.A., Azeem, F., Abbas, A., Joyia, F.A., Li, H., and Dababat, A.A. (2017) Transgenic
502 Strategies for Enhancement of Nematode Resistance in Plants. *Frontiers in Plant*
503 *Science*, **8**, 1–13.

504 de Almeida Engler, J. and Gheysen, G. (2013) Nematode-induced endoreduplication in plant
505 host cells: why and how? *Molecular Plant-Microbe Interactions*, **26**, 17–24.

506 Banerjee, S., Banerjee, A., Gill, S.S., Gupta, O.P., Dahuja, A., Jain, P.K., and Sirohi, A.
507 (2017) RNA Interference: A Novel Source of Resistance to Combat Plant Parasitic
508 Nematodes. *Frontiers in Plant Science*, **8**:834, doi: 10.3389/fpls.2017.00834.

509 Bastet, A., Zafirov, D., Giovinazzo, N., Guyon-Debast, A., Nogué, F., Robaglia, C., and
510 Gallois, J.L. (2019) Mimicking natural polymorphism in eIF4E by CRISPR-Cas9 base
511 editing is associated with resistance to potyviruses. *Plant Biotechnology Journal*, **17**,
512 1736–1750.

513 Blanc-Mathieu, R., Perfus-Barbeoch, L., Aury, J.-M.M., Da Rocha, M., Gouzy, J., Sallet, E.,
514 et al. (2017) Hybridization and polyploidy enable genomic plasticity without sex in the
515 most devastating plant-parasitic nematodes. *PLoS Genetics*, **13**, e1006777.

516 Blok, V.C., Jones, J.T., Phillips, M.S., and Trudgill, D.L. (2008) Parasitism genes and host
517 range disparities in biotrophic nematodes: The conundrum of polyphagy versus
518 specialisation. *Bioessays*, **30**, 249–259.

519 Cabrera, J., Bustos, R., Favery, B., Fenoll, C., and Escobar, C. (2014) NEMATIC: a simple

- 520 and versatile tool for the in silico analysis of plant-nematode interactions. *Molecular*
521 *Plant Pathology*, **15**, 627–636.
- 522 Cabrera, J., Olmo, R., Ruiz-Ferrer, V., Abreu, I., Hermans, C., Martinez-Argudo, I., et al.
523 (2018) A Phenotyping Method of Giant Cells from Root-Knot Nematode Feeding Sites
524 by Confocal Microscopy Highlights a Role for CHITINASE-LIKE 1 in Arabidopsis.
525 *International Journal of Molecular Sciences*, **19**, 429.
- 526 Caillaud, M.-C., Abad, P., and Favery, B. (2008) Cytoskeleton reorganization. *Plant*
527 *Signaling & Behavior*, **3**, 816–818.
- 528 Caillaud, M.-C.C. and Favery, B. (2016) In Vivo Imaging of Microtubule Organization in
529 Dividing Giant Cell. In: *Methods in Molecular Biology* (Caillaud, M.-C., ed) , pp. 137–
530 144. New York: Springer New York.
- 531 Castagnone-Sereno, P. (2006) Genetic variability and adaptive evolution in parthenogenetic
532 root-knot nematodes. *Heredity*, **96**, 282–289.
- 533 Chaudhari, P., Ahmed, B., Joly, D.L., and Germain, H. (2014) Effector biology during
534 biotrophic invasion of plant cells. *Virulence*, **5**, 703–709.
- 535 Cox, D.E., Dyer, S., Weir, R., Cheseto, X., Sturrock, M., Coyne, D., et al. (2019) ABC
536 transporter genes ABC-C6 and ABC-G33 alter plant-microbe-parasite interactions in the
537 rhizosphere. *Scientific Reports*, **9**, 19899.
- 538 Danchin, E.G.J., Rosso, M.-N.N., Vieira, P., de Almeida-Engler, J., Coutinho, P.M.,
539 Henrissat, B., and Abad, P. (2010) Multiple lateral gene transfers and duplications have
540 promoted plant parasitism ability in nematodes. *Proc Natl Acad Sci U S A*, **107**, 17651–
541 17656.
- 542 Dong, O.X. and Ronald, P.C. (2019) Genetic Engineering for Disease Resistance in Plants:
543 Recent Progress and Future Perspectives. *Plant Physiology*, **180**, 26–38.
- 544 Doyle, E.A. and Lambert, K.N. (2003) *Meloidogyne javanica* chorismate mutase 1 alters plant

- 545 cell development. *Mol Plant Microbe Interact*, **16**, 123–131.
- 546 Elling, A. a (2013) Major emerging problems with minor meloidogyne species.
547 *Phytopathology*, **103**, 1092–1102.
- 548 Engelhardt, S., Stam, R., and Hückelhoven, R. (2018) Good Riddance? Breaking Disease
549 Susceptibility in the Era of New Breeding Technologies. *Agronomy*, **8**, 114.
- 550 Escobar, C., Barcala, M., Cabrera, J., and Fenoll, C. (2015) Overview of Root-Knot
551 Nematodes and Giant Cells. In: *Advances in Botanical Research* , pp. 1–32.
- 552 Favery, B., Quentin, M., Jaubert-Possamai, S., and Abad, P. (2016) Gall-forming root-knot
553 nematodes hijack key plant cellular functions to induce multinucleate and hypertrophied
554 feeding cells. *Journal of Insect Physiology*, **84**, 60–69.
- 555 Gleason, C., Polzin, F., Habash, S.S., Zhang, L., Utermark, J., Grundler, F.M.W., and
556 Elashry, A. (2017) Identification of two Meloidogyne hapla genes and an investigation
557 of their roles in the plant-nematode interaction. *Molecular Plant-Microbe Interactions*,
558 **30**, 101–112
- 559 Hewezi, T. and Baum, T.J. (2013) Manipulation of Plant Cells by Cyst and Root-Knot
560 Nematode Effectors. *Molecular Plant-Microbe Interactions*, **26**, 9–16.
- 561 Holbein, J., Franke, R.B., Marhavý, P., Fujita, S., Górecka, M., Sobczak, M., et al. (2019)
562 Root endodermal barrier system contributes to defence against plant - parasitic cyst and
563 root - knot nematodes. *The Plant Journal*, **100**, 221–236.
- 564 Huang, G.Z., Allen, R., Davis, E.L., Baum, T.J., and Hussey, R.S. (2006) Engineering broad
565 root-knot resistance in transgenic plants by RNAi silencing of a conserved and essential
566 root-knot nematode parasitism gene. *Proceedings of the National Academy of Sciences of
567 the United States of America*, **103**, 14302–14306.
- 568 Jaouannet, M., Nguyen, C.-N., Quentin, M., Jaubert-Possamai, S., Rosso, M.-N., and Favery,
569 B. (2018) In situ Hybridization (ISH) in Preparasitic and Parasitic Stages of the Plant-

- 570 parasitic Nematode *Meloidogyne* spp. *Bio-Protocol*, **8**, 1–13.
- 571 Jones, J.T., Haegeman, A., Danchin, E.G.J.J., Gaur, H.S., Helder, J., Jones, M.G.K.K., et al.
572 (2013) Top 10 plant-parasitic nematodes in molecular plant pathology. *Molecular Plant*
573 *Pathology*, **14**, 946–961.
- 574 Karszen, G. and Moens, M. (1983) Root-knot nematodes. In: *Plant nematology* , pp. 59–90.
575 Wallingford: CABI.
- 576 Kiewnick, S., Dessimoz, M., and Franck, L. (2009) Effects of the Mi-1 and the N root-knot
577 nematode-resistance gene on infection and reproduction of *Meloidogyne enterolobii* on
578 tomato and pepper cultivars. *Journal of nematology*, **41**, 134–9.
- 579 Koutsovoulos, G.D., Pouillet, M., Elashry, A., Kozłowski, D.K.L., Sallet, E., Da Rocha, M., et
580 al. (2020) Genome assembly and annotation of *Meloidogyne enterolobii*, an emerging
581 parthenogenetic root-knot nematode. *Scientific Data*, **7**, 324.
- 582 Landry, D., González - Fuente, M., Deslandes, L., and Peeters, N. (2020) The large, diverse,
583 and robust arsenal of *Ralstonia solanacearum* type III effectors and their in planta
584 functions. *Molecular Plant Pathology*, **21**, 1377–1388.
- 585 Lange, M., Yellina, A.L., Orashakova, S., and Becker, A. (2013) Virus-Induced Gene
586 Silencing (VIGS) in Plants: An Overview of Target Species and the Virus-Derived
587 Vector Systems. In: *Methods in Molecular Biology* , pp. 1–14. Humana Press Inc.
- 588 Langner, T., Kamoun, S., and Belhaj, K. (2018) CRISPR Crops: Plant Genome Editing
589 Toward Disease Resistance. *Annual Review of Phytopathology*, **56**, 479–512.
- 590 Lin, B., Zhuo, K., Chen, S., Hu, L., Sun, L., Wang, X., et al. (2016) A novel nematode
591 effector suppresses plant immunity by activating host reactive oxygen species-
592 scavenging system. *New Phytologist*, **209**, 1159–1173.
- 593 Lin, B., Zhuo, K., Wu, P., Cui, R., Zhang, L.-H., and Liao, J. (2013) A novel effector protein,
594 MJ-NULG1a, targeted to giant cell nuclei plays a role in *Meloidogyne javanica*

- 595 parasitism. *Molecular plant-microbe interactions*, **26**, 55–66.
- 596 Liu, D., Shi, L., Han, C., Yu, J., Li, D., and Zhang, Y. (2012) Validation of Reference Genes
597 for Gene Expression Studies in Virus-Infected *Nicotiana benthamiana* Using
598 Quantitative Real-Time PCR. *PLoS ONE*, **7**, e46451.
- 599 Lunt, D.H., Kumar, S., Koutsovoulos, G., and Blaxter, M.L. (2014) The complex hybrid
600 origins of the root knot nematodes revealed through comparative genomics. *PeerJ*, **2**,
601 e356.
- 602 Mantelin, S., Bellafiore, S., and Kyndt, T. (2017) *Meloidogyne graminicola*: a major threat
603 to rice agriculture. *Molecular Plant Pathology*, **18**, 3–15.
- 604 Mejias, J., Bazin, J., Truong, N., Chen, Y., Marteu, N., Bouteiller, N., et al. (2020) The
605 root - knot nematode effector MiEFF18 interacts with the plant core spliceosomal
606 protein SmD1 required for giant cell formation. *New Phytologist*, **in press**, doi:
607 10.1111/nph.17089.
- 608 Mejias, J., Truong, N.M., Abad, P., Favery, B., and Quentin, M. (2019) Plant Proteins and
609 Processes Targeted by Parasitic Nematode Effectors. *Frontiers in Plant Science*, **10**, 970.
- 610 Mitchum, M.G., Hussey, R.S., Baum, T.J., Wang, X., Elling, A.A., Wubben, M., and Davis,
611 E.L. (2013) Nematode effector proteins: an emerging paradigm of parasitism. *New*
612 *Phytologist*, **199**, 879–894.
- 613 Mitchum, M.G., Wang, X., Wang, J., and Davis, E.L. (2012) Role of Nematode Peptides and
614 Other Small Molecules in Plant Parasitism. *Annual Review of Phytopathology*, **50**, 175–
615 195.
- 616 Muhire, B.M., Varsani, A., and Martin, D.P. (2014) SDT: A Virus Classification Tool Based
617 on Pairwise Sequence Alignment and Identity Calculation. *PLoS ONE*, **9**, e108277.
- 618 Nguyen, C.-N., Perfus-Barbeoch, L., Quentin, M., Zhao, J., Magliano, M., Marteu, N., et al.
619 (2018) A root-knot nematode small glycine and cysteine-rich secreted effector,

- 620 MiSGCR1, is involved in plant parasitism. *New Phytologist*, **217**, 687–699.
- 621 O’Connell, R.J. and Panstruga, R. (2006) Tete a tete inside a plant cell: establishing
622 compatibility between plants and biotrophic fungi and oomycetes. *New Phytologist*, **171**,
623 699–718.
- 624 Olmo, R., Cabrera, J., Díaz-Manzano, F.E., Ruiz-Ferrer, V., Barcala, M., Ishida, T., et al.
625 (2020) Root - knot nematodes induce gall formation by recruiting developmental
626 pathways of post - embryonic organogenesis and regeneration to promote transient
627 pluripotency. *New Phytologist*, **227**, 200–215.
- 628 Opperman, C.H., Bird, D.M., Williamson, V.M., Rokhsar, D.S., Burke, M., Cohn, J., et al.
629 (2008) Sequence and genetic map of *Meloidogyne hapla*: A compact nematode genome
630 for plant parasitism. *Proc Natl Acad Sci U S A*, **105**, 14802–14807.
- 631 P. T. Y. Dinh (2015) Plant-nematode interactions and the application of RNA interference for
632 controlling root-knot nematodes. *PhD*, **3**, 54–67.
- 633 Peeters, N., Carrère, S., Anisimova, M., Plener, L., Cazalé, A.-C., and Genin, S. (2013)
634 Repertoire, unified nomenclature and evolution of the Type III effector gene set in the
635 *Ralstonia solanacearum* species complex. *BMC Genomics*, **14**, 859.
- 636 Quentin, M., Abad, P., and Favery, B. (2013) Plant parasitic nematode effectors target host
637 defense and nuclear functions to establish feeding cells. *Frontiers in Plant Science*, **4**, 53.
- 638 Rancurel, C., van Tran, T., Elie, C., and Hilliou, F. (2019) SATQPCR: Website for statistical
639 analysis of real-time quantitative PCR data. *Molecular and Cellular Probes*, **46**, 101418.
- 640 Rodiuc, N., Vieira, P., Banora, M.Y., and de Almeida Engler, J. (2014) On the track of
641 transfer cell formation by specialized plant-parasitic nematodes. *Frontiers in Plant*
642 *Science*, **5**, 1–14.
- 643 Roux, B., Bolot, S., Guy, E., Denancé, N., Lautier, M., Jardinaud, M.-F., et al. (2015)
644 Genomics and transcriptomics of *Xanthomonas campestris* species challenge the concept

- 645 of core type III effectome. *BMC Genomics*, **16**, 975.
- 646 Rutter, W.B., Hewezi, T., Abubucker, S., Maier, T.R., Huang, G., Mitreva, M., et al. (2014)
- 647 Mining Novel Effector Proteins from the Esophageal Gland Cells of *Meloidogyne*
- 648 *incognita*. *Molecular plant-microbe interactions*, **27**, 965–974.
- 649 van Schie, C.C.N. and Takken, F.L.W. (2014) Susceptibility Genes 101: How to Be a Good
- 650 Host. *Annual Review of Phytopathology*, **52**, 551–581.
- 651 Schmitt-Keichinger, C. (2019) Manipulating Cellular Factors to Combat Viruses: A Case
- 652 Study From the Plant Eukaryotic Translation Initiation Factors eIF4. *Frontiers in*
- 653 *Microbiology*, **10**:17. doi: 10.3389/fmicb.2019.00017
- 654 Singh, S.K., Hodda, M., and Ash, G.J. (2013) Plant-parasitic nematodes of potential
- 655 phytosanitary importance, their main hosts and reported yield losses. *EPPO Bulletin*, **43**,
- 656 334–374.
- 657 Somvanshi, V.S., Tathode, M., Shukla, R.N., and Rao, U. (2018) Nematode Genome
- 658 Announcement: A Draft Genome for Rice Root-Knot Nematode, *Meloidogyne*
- 659 *graminicola*. *Journal of Nematology*, **50**, 111–116.
- 660 Susič, N., Koutsovoulos, G.D., Riccio, C., Danchin, E.G.J., Blaxter, M.L., Lunt, D.H., et al.
- 661 (2020) Genome sequence of the root-knot nematode *Meloidogyne luci*. *Journal of*
- 662 *Nematology*, **52**, e2020-25.
- 663 Tomalova, I., Iachia, C., Mulet, K., and Castagnone-Sereno, P. (2012) The map-1 gene family
- 664 in root-knot nematodes, *Meloidogyne* spp.: a set of taxonomically restricted genes
- 665 specific to clonal species. *PloS one*, **7**, e38656.
- 666 Toruño, T.Y., Stergiopoulos, I., and Coaker, G. (2016) Plant-Pathogen Effectors: Cellular
- 667 Probes Interfering with Plant Defenses in Spatial and Temporal Manners. *Annual Review*
- 668 *of Phytopathology*, **54**, 419–441.
- 669 Truong, N.M., Nguyen, C.-N., Abad, P., Quentin, M., and Favery, B. (2015) Function of

- 670 Root-Knot Nematode Effectors and Their Targets in Plant Parasitism. In: *Elsevier*
671 (Escobar,C. and Fenoll,C., eds) , pp. 293–324. Academic Press.
- 672 Velasquez, A., Chakravarthy, S., and Martin, G.B. (2009) Virus-induced Gene Silencing
673 (VIGS) in *Nicotiana benthamiana* and Tomato. *Journal of Visualized Experiments*, 28:
674 1292. doi: 10.3791/1292.
- 675 Wang, X., Xue, B., Dai, J., Qin, X., Liu, L., Chi, Y., et al. (2018) A novel Meloidogyne
676 incognita chorismate mutase effector suppresses plant immunity by manipulating the
677 salicylic acid pathway and functions mainly during the early stages of nematode
678 parasitism. *Plant Pathology*, **67**, 1436–1448.
- 679 Yamaguchi, Y.L., Suzuki, R., Cabrera, J., Nakagami, S., Sagara, T., Ejima, C., et al. (2017)
680 Root-Knot and Cyst Nematodes Activate Procambium-Associated Genes in Arabidopsis
681 Roots. *Frontiers in Plant Science*, **8**, 1195.
- 682 Yang, Y., Jittayasothorn, Y., Chronis, D., Wang, X., Cousins, P., and Zhong, G.-Y. (2013)
683 Molecular characteristics and efficacy of 16D10 siRNAs in inhibiting root-knot
684 nematode infection in transgenic grape hairy roots. *PloS one*, **8**, e69463.
- 685 Zhang, L., Davies, L.J., and Elling, A. a (2015) A Meloidogyne incognita effector is imported
686 into the nucleus and exhibits transcriptional activation activity in planta. *Molecular Plant*
687 *Pathology*, **16**, 48–60.

688

689 **Figure legends**

690

691 **Figure 1** Effector 18 (EFF18) is a conserved effector in root-knot nematodes. (a)
692 Phylogenetic tree and schematic diagram of root-knot nematode EFF18 protein sequences.
693 The tree scale corresponds to the number of substitutions per site based on the amino-acid
694 matrix (JTT). In the schematic diagram of EFF18 proteins, the predicted secretion signal

695 peptide (SP; grey boxes), the aspartic acid and glutamic acid (D-E)-rich region (red boxes),
696 the lysine (K)-rich C-terminal region (blue boxes) and the nuclear mono- (purple boxes) or
697 bi- (orange boxes) partite localisation signals (NLS) are shown. EFF18 proteins from the
698 closest group to MiEFF18a carry one mono- and one bipartite NLS, whereas the most
699 divergent copies have only a single monopartite NLS. (b) MiEFF18 localised to the nucleus
700 and nucleolus of plant cells. The MiEFF18 sequence was fused to that encoding GFP in an N-
701 or C-terminal position and expressed in *N. benthamiana* leaves by agroinfiltration. GFP was
702 used as a control and gave fluorescence in the cytoplasm and the nucleus (n), but not the
703 nucleolus (arrowhead). Bars = 10 μ m. (c) Pairwise sequence identity matrix for RKN EFF18
704 protein sequences.

705

706 **Figure 2** RKN EFF18s are specifically expressed in the subventral glands. *In situ*
707 hybridisation, showing EFF18 transcripts in the subventral glands of J2s of *M. incognita*, *M.*
708 *enterolobii* and *M. arenaria*, respectively. A sense probe for the MeEFF18 transcript was used
709 as a negative control. SvG, subventral glands. Bar = 50 μ m.

710

711 **Figure 3** Conserved SmD1 proteins are targeted by EFF18. (a) MAFFT protein sequence
712 alignment of the *S. lycopersicum* (Sl), *N. benthamiana* (Nb) and *A. thaliana* (At) SmD1
713 proteins. (b) Schematic representation of Sm1 and Sm2 motif in SmD1 proteins. (c) GFP-
714 AtSmD1b and GFP-SlSmD1a accumulate in the nucleus and particularly in the nucleolus
715 when transiently expressed in *N. benthamiana* epidermal leaf cells. GFP was used as a
716 nucleocytoplasmic control. n= nucleoplasm; Black arrows show nucleolus. Bars = 5 μ m. (d)
717 Pairwise yeast two-hybrid assays showed that the MiEFF18 and MeEFF18 proteins were able
718 to interact with the SmD1 proteins of *A. thaliana*, *S. lycopersicum* and *N. benthamiana*. We
719 used MiEFF18 and MiEFF16 as a positive and negative control, respectively. Diploid yeasts
720 containing the bait and prey plasmids carrying controls, effectors or SmD1 were serially

721 diluted and spotted on plates. The 10⁻² dilution is shown. SD-WL corresponds to the non-
722 selective medium without tryptophan (W) and leucine (L). Only yeasts carrying a protein-
723 protein interaction can survive on the SD-WLH (H, histidine) + 0.5 mM 3-aminotriazole (3-
724 AT) selective medium.

725

726 **Figure 4** The silencing of *SmD1* genes by VIGS affects susceptibility to *M. incognita* in *S.*
727 *lycopersicum*. (a) Timeline used for the VIGS experiments in *S. lycopersicum*. (b) RT-qPCR
728 demonstrating the effective silencing of *SlSmD1* in TRV-*SlSmD1* line when compared to the
729 control TRV-GFP. RPN7 was used for data normalisation. (c) Infection test on tomato plants
730 in which *SmD1* was silenced (TRV-*SlSmD1*) and control tomato plants (TRV-GFP). Females
731 producing egg masses were counted seven weeks after inoculation with 150 *M. incognita* J2s
732 per plant. Statistical significance was determined on the basis of three independent biological
733 replicates, by Kruskal-Wallis tests. Clearly significant differences were observed between
734 TRV-GFP control and TRV-*SmD1* plants (* $p \leq 0.05$).

735

736 **Figure 5** The silencing of *SmD1* genes by VIGS affects susceptibility to *M. incognita* in *N.*
737 *benthamiana*. (a) Timeline used for VIGS experiment in *N. benthamiana*. (b) *N. benthamiana*
738 plants with silenced *SmD1* genes (TRV-*SmD1*, right panel) and TRV2-empty control plants
739 (TRV-empty, left panel), showing some developmental defects of the leaves (upper panel)
740 and a shorter root system (lower panel). Red arrow point-out galls on these pictures. (c) RT-
741 qPCR showing that the *NbSmD1b* gene, the most strongly expressed and closest orthologue
742 to the *SlSmD1* gene, was effectively silenced. The data shown are the means of three
743 independent biological replicates. EF1a and actin were used for data normalisation. (d)
744 Infection test on *N. benthamiana* control plants (TRV-empty) and plants in which *SmD1* was
745 silenced (TRV-*SlSmD1*). Galls were counted and root weight was measured two weeks after

746 inoculation with 200 *M. incognita* J2s per plant. Statistical significance was determined on the
747 basis of three independent biological replicates, by Kruskal-Wallis tests. Clear significant
748 differences were found between the TRV-GFP control and the TRV-SmD1 plants (* $p \leq 0.05$;
749 ** $p \leq 0.01$).

750

751 **Figure 6** *SmD1* plays an important role in the formation of giant cells. (a) The filiform
752 J2s/swollen juveniles (Js) ratio obtained by fuchsine acid staining in the *N. benthamiana* root
753 system with (TRV-SmD1) and without (TRV-empty) silencing with the TRV-SISmD1
754 construct, following infection with *M. incognita*. (b) Galls of negative control plants and
755 plants with SmD1 silencing collected two weeks post infection for measurement of the area
756 of giant cells (dotted line) by the BABB clearing method (Cabrera et al., 2018). The biggest
757 giant cell measured is shown by a surrounding dashed white line. Bar = 100 μm . (c) Box-and-
758 whisker plot of giant cell size (μm^2) measurements (n = 32 and 26 galls).

759

760 **Supporting information**

761

762 **Figure S1** Identified EFF18 sequences in RKN species.

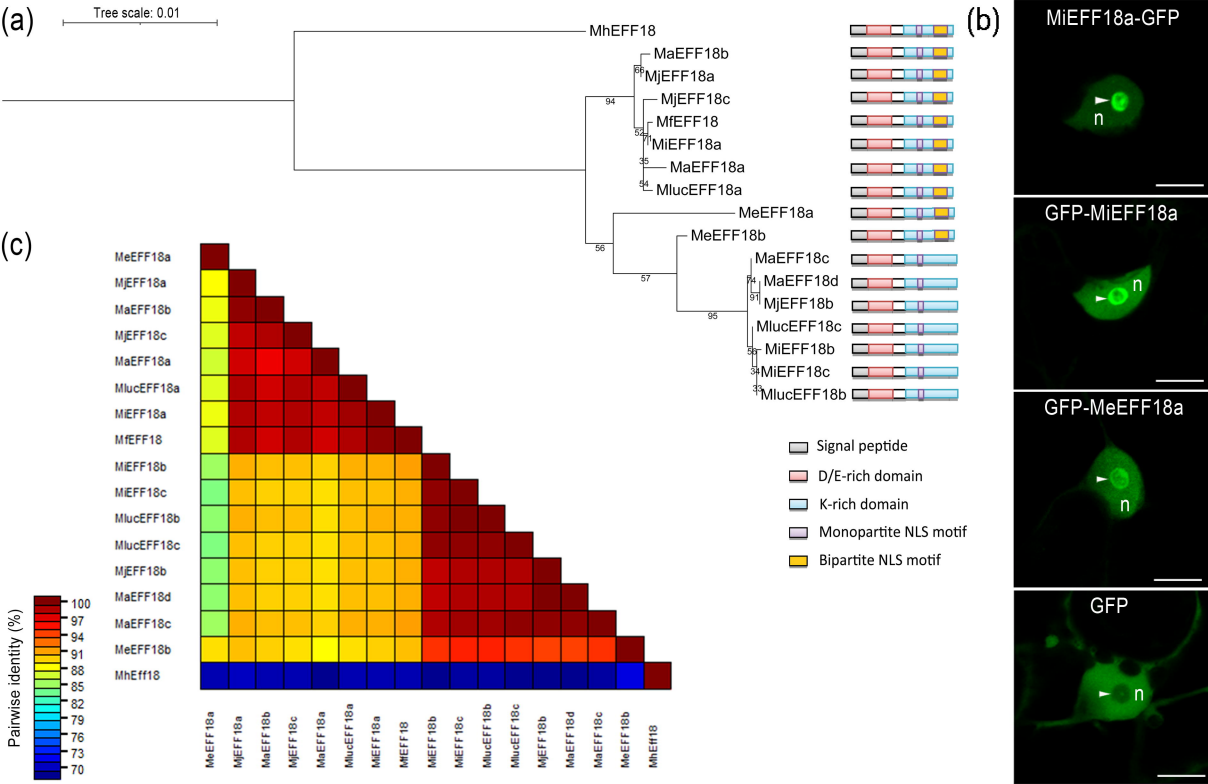
763 **Figure S2** EFF18 is a conserved RKN effector.

764 **Figure S3** Tomato phenotypes associated with VIGS of *SISmD1* genes.

765 **Figure S4** Semi-quantitative RT-PCR expression analysis of *NbSmD1s* in *N. benthamiana*
766 roots VIGS experiments.

767 **Table S1** Sequences used in this study and accession numbers

768 **Table S2** Primers used in this study



M. incognita



M. arenaria



M. enterolobii



